JACS
JOURNAL OF THE AMERICAN CHEMICAL SOCIETY
Communication
Cite This: J. Am. Chem. Soc. XXXX, XXX, XXX−XXX
pubs.acs.org/JACS

Shock Wave Energy Absorption in Metal−Organic Framework

Xuan Zhou, Yu-Run Miao,[†] William L. Shaw,[‡] Kenneth S. Suslick,* and Dana D. Dlott*

Department of Chemistry, University of Illinois at Urbana−Champaign, Urbana, Illinois 61801, United States

Supporting Information

ABSTRACT: Recent investigations into the mechanical properties and mechanochemical reactions of metal−organic frameworks (MOFs) have suggested the potential for energy dissipation by multiple mechanisms. Although the possibility of efficient multifunctional shock dissipation by MOFs was suggested by static high pressure studies, there is little known about MOFs under shock compression. Here, we measure the attenuation of shock wave by the MOF denoted zeolitic-imidazolate framework (ZIF-8) in its desolvated, porous state. We find that shock wave dissipation by ZIF-8 occurred by multiple processes: powder compaction, nanopore-collapse, and chemical bond-breakage. The shock energy absorbance in ZIF-8 is proportional to ZIF-8 thickness, allowing the prediction of the thickness of MOF layer needed to attenuate shock waves to a desired lower energy. Compared with PMMA, often used as a standard, ZIF-8 attenuates 7 times more shock energy per unit mass for impacts at a lower velocity of 0.75 km/s and 2.5 times more at a higher velocity of 1.6 km/s. This research illustrates how to improve the ability to attenuate shock waves for personnel and equipment protection by engineering multifunctionality into the shock wave absorbing armor material.

Metal−organic frameworks have shown promising potential for mechanical energy attenuation in recent investigations using static high pressure.[1−5] Within the limit of reversible structural deformation (i.e., elastic limit), MOFs can store energy up to 60 J/g.[2,4,5] Under stronger compression, MOFs undergo plastic deformations such as amorphization[6] and nanopore-collapse,[7] leading to more efficient mechanical energy absorption. A recent nanoindentation study has reported that UiO series MOF, when compressed beyond its elastic limit, can absorb 4 kJ/g at GPa-scale pressures,[1] which, gram-for-gram, is comparable to the energy density[8] of TNT (4.18 kJ/g). Recently, another mechanism for mechanical energy absorption, endothermic chemical bond breakage, was reported in UiO-66.[9]

Although the efficient multifunctional energy absorption by MOFs has been suggested by static high pressure investigations, there is little known about the MOFs under shock compression for their potential application as protective materials. A reactive force field simulation on MOF-5[10] and our previous experimental observation on ZIF-8[11] reported the shock-induced structural collapse accompanied by amorphization and endothermic bond-scission at different loading pressures. Yet, the processes and the efficiency of shock energy absorption by MOFs remains to be investigated. In this article, we studied the attenuation of energy in a MOF (ZIF-8) film under dynamic shock loading. Compared with PMMA, often used as a shock absorption standard,[12,13] ZIF-8 attenuates 2.5 to 7 times more shock energy per unit mass, depending on impact velocity. We attribute this outstanding performance to the multiple shock attenuation mechanisms that include powder compaction, nanopore-collapse and chemical bond-breakage.

Rhombic dodecahedral ZIF-8 microcrystals of uniform size were synthesized according to previous literature.[14] Details about the polymer-bonded ZIF-8 film preparation are available in the Supporting Information. The film thickness was varied from 4 to 110 μm. An SEM image of ZIF-8 film (Figure 1a) shows that ZIF-8 crystals of about 2 μm are loosely piled with considerable free volume. Figure 1b shows the structure of the ZIF-8 unit cell. The nanoporosity accounts for about 50% of the cell volume.[15] Figure 1c illustrates the ZIF-8 molecular structure where each Zn atom is coordinated by four N atoms from imidazolate rings.[16]

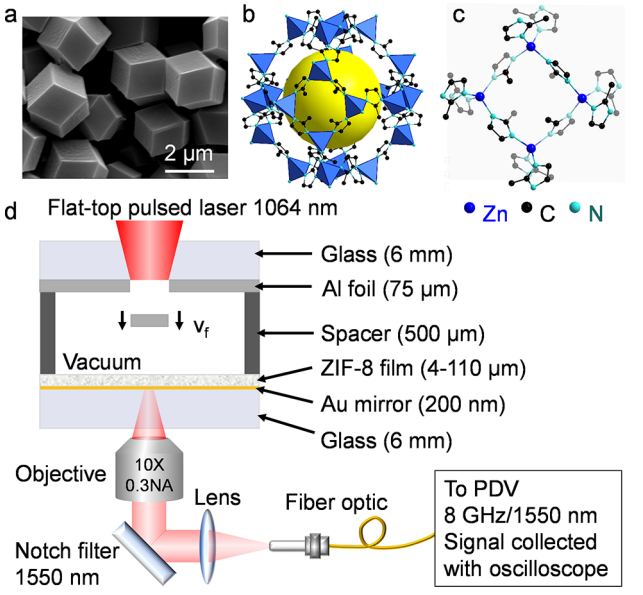

Figure 1. ZIF-8 structures and shock apparatus. (a) SEM image of single crystal powder. (b) Structure of unit crystal cell. Yellow sphere is a visual guide to indicate the internal void volume. (c) Structure showing the Zn atoms at the vertices and the coordinating N atoms from the 2-methylimidazolate rings. (d) Schematic of the shock apparatus and sample with photon Doppler velocimeter (PDV).

Received: December 2, 2018
Published: January 31, 2019

DOI: 10.1021/jacs.8b12905
J. Am. Chem. Soc. XXXX, XXX, XXX−XXX

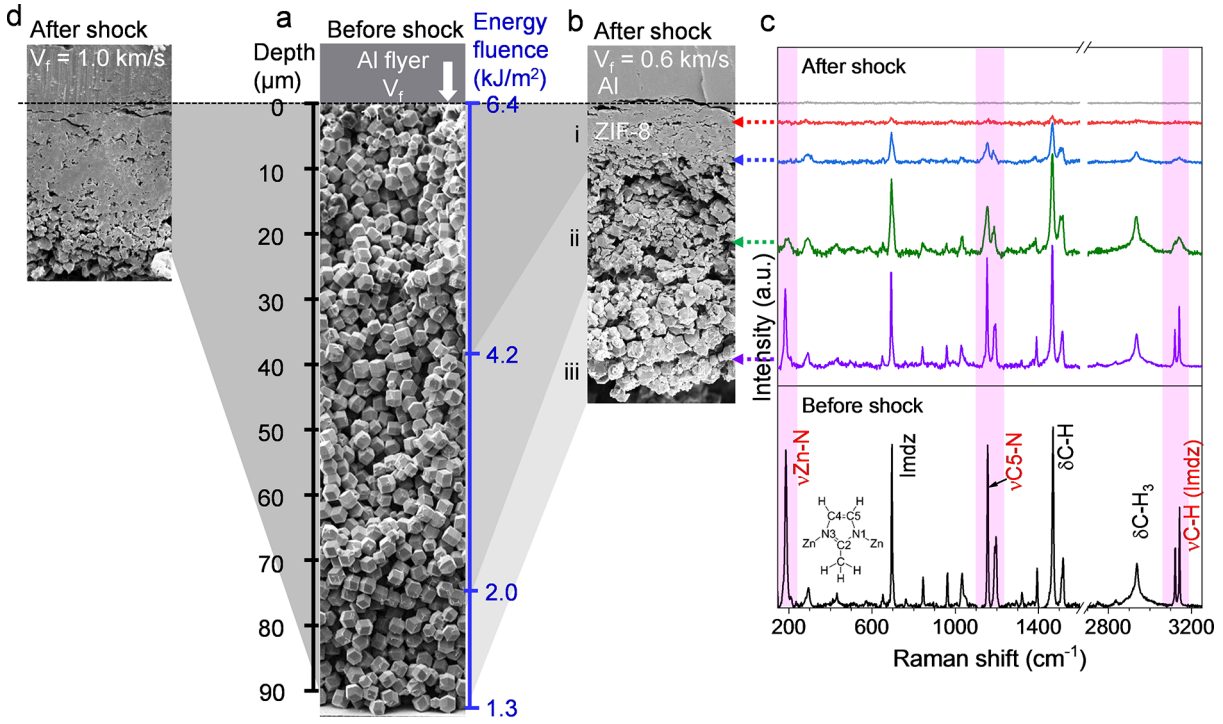

Figure 2. Cross-sectional topographic characterization and spectroscopic analysis before and after shock compression. (a) SEM side-view of a 92 μm-thick ZIF-8 film before shock. (b) SEM side-view of the ZIF-8 film after a 0.6 km/s impact. (c) Confocal Raman spectra in different regions along the direction of shock propagation in the shocked ZIF-8 film. The detecting regions were ~1 μm in diameter. ν, stretching; δ, bending; Imdz, imidazolate. The colored arrows indicate the part of the shocked ZIF-8 where each spectrum was obtained. (d) SEM side-view of the ZIF-8 film after impact at 1.0 km/s.

Figure 1d depicts the apparatus for shock compression.[17,18] An Al flyer plate 75 μm thick and 500 μm in diameter is launched by a single pulse of the uniform beam of 1064 nm laser, which produces up to 2.5 J/pulse in a 10 or 20 ns pulse.[18,19] The flyer plate velocity could be varied from 0.6 to 1.9 km/s. To stabilize launch transients, the flyer plate travels 500 μm in vacuum before impacting the ZIF-8 film. The impact geometry, sample thickness, and probe lasers were arranged so the shock induced was purely one-dimensional.[18,19] The shock wave rises the pressure in ZIF-8 film to 0.9−4.6 GPa within 2 ns (Supporting Information). After passing through the ZIF-8 attenuation layer, the shock enters a borosilicate glass window with an ultrathin, nonperturbative Au mirror. The motion of this mirror, corresponding to the motion of the ZIF-8/glass interface, is measured by photon Doppler velocimetry (PDV).[20] Knowing the velocity history of the mirror and the Hugoniot of the borosilicate glass window, using methods described elsewhere[21] and in Supporting Information, it is possible to determine the shock energy flux (energy per unit area per unit time) and energy fluence (time-integrated flux) of the shock exiting the ZIF-8. During the impact, the ZIF-8 film adheres to the flyer plate, and after the subsequent rebound, the ZIF-8 debonds from the glass or Au-coated glass substrate. Consequently and remarkably, the flyer plate with its transferred ZIF-8 coating can be recovered for post-mortem analysis (Figure S2).

We collected the ZIF-8-attached Al plates after impact and made a cut through the center of the ZIF-8 coating with a sharp blade that did not noticeably damage the recovered coating (Refer to Figure S3 for ZIF-8 film cross-section). We carried out topographic characterization with scanning electron microscopy (SEM) and micro-Raman spectroscopy on ZIF-8 film cross sections before and after shock compression. Figure 2a shows the cross-section of a 92 μm thick ZIF-8 film before shock. After shock compression at lower impact velocity of 0.6 km/s (Figure 2b), we can identify three zones produced by the ZIF-8 film as the dynamically attenuating shock propagates through the film. Region (i) is nearest to the shock entry plane where the shock energy is largest. Region (i) is a fully compacted region where single crystals cannot be recognized. Region (ii), created by the shock attenuated by passage through Region (i) is the pore-collapse region, where crystals are clearly smaller in dimension than before shock. Region (iii) is powder compaction region, where the powder is compacted but the crystals appear undamaged.

The powder compaction and pore-collapse suggest a shock-induced structural transformation in the ZIF-8 film. To better understand the nature of this shock-attenuating transformation, we compared the confocal Raman spectra on the ZIF-8 before and after shock (Figure 2c). In the powder-compaction region, the postmortem spectrum (violet) was indistinguishable from the unshocked spectrum (black), so the shock compression compacted the powder but left the unit cell structure unchanged. The Raman spectrum in the pore-collapse region (green) shows some broadening of the vibrational transitions. The Raman intensity of the Zn−N stretching mode[22] at 183 cm^{-1} shows a significant drop. These observations are consistent with pore-collapse accompanied by breakage of some Zn−N bonds. The spectrum at the interface between the pore-collapse and fully compacted regions (blue) shows the Zn−N mode disappears, indicating the breakage of Zn−N coordination bond, and the C5−N and C−H (Imidazolate) modes at 1155 and 3142 cm^{-1}, respectively, are broadened and have lost intensity. The spectrum in the

DOI: 10.1021/jacs.8b12905
J. Am. Chem. Soc. XXXX, XXX, XXX−XXX

fully compacted region (red) shows the C−H (Imidazolate) bonds are broken while the imidazole ring itself is recognizable.

From the discussions above, we conclude that ZIF-8 films can dissipate shock wave in three mechanisms: powder-compaction, pore-collapse, and chemical bond-breakage. These mechanisms appear at different distances along the shock propagation axis, as shown in Figure 2b,c, indicating the existence of distinct threshold energies for each process. The threshold energies can be estimated based on the initial depths of boundaries between two neighboring regions and the shock energy measured at these depths.

To determine the threshold for chemical bond-breakage, we collected a sample that was almost fully compacted (Figure 2d). We can deduce a contraction factor of $C \approx 4$ for the full compaction of ZIF-8 film from

$$C = l_0/l \tag{1}$$

where l_0 and l are the thicknesses of fully compacted region before and after impact, respectively. This factor is not obviously affected by the impact velocity (Figure S4). After a slower impact at 0.6 km/s, the fully compacted region was ~10 μm thick (Figure 2b). The original thickness of this region was calculated as 40 μm. The shock energy fluence measured after passing through a 40 μm-thick ZIF-8 film was 4.2 kJ/m^2 (Figure S5). Therefore, the threshold for bond-breakage is about 4.2 kJ/m^2.

The threshold for nanopore-collapse was determined based on an approximation that the volume decrease in the powder-compaction region is small enough to be ignored compared to the fully compacted and pore-collapse regions. After impact at 0.6 km/s (Figure 2b), the powder compaction region was 17 μm thick. The initial depth of the boundary between pore-collapse and powder compaction region was 92−17 = 75 μm. The shock energy fluence measured after 75 μm-thick ZIF-8 film was 2.0 kJ/m^2. Consequently, the threshold for pore-collapse is about 2.0 kJ/m^2.

Having observed the multiple mechanisms of shock energy dissipation in ZIF-8 film and estimated their thresholds, we wish to better understand shock propagation in MOF and quantify the energy attenuation as a shock propagates through ZIF-8. To this end, we have also measured the energy flux of shocks exiting ZIF-8 layers from 4 to 110 μm thick (Figure S7). We write the shock energy transmittance T of ZIF-8 film as (Figure S9a)

$$T = f/f_0 \tag{2}$$

where f_0 is the incident shock energy flux. To determine the incident flux, we looked at the shock exiting an ultrathin, practically nonattenuating 4 μm-thick ZIF-8 layer. The parameter f is the energy flux transmitted through different thicknesses of ZIF-8 film. The shock energy absorbance A can be written as

$$A = -\log_{10}(f/f_0) \tag{3}$$

Figure 3 demonstrates that the shock energy absorbance is proportional to the thickness of ZIF-8 film. The slope indicates the shock absorption coefficient in MOF and it saturates as the impact velocity increases. Despite a smaller absorbance at higher impact velocities (Figure 3), the total amount of absorbed shock energy increases as shown in Figure 4.

From the perspective of armor materials, weight is always a concern in addition to the shock wave attenuation. Therefore,

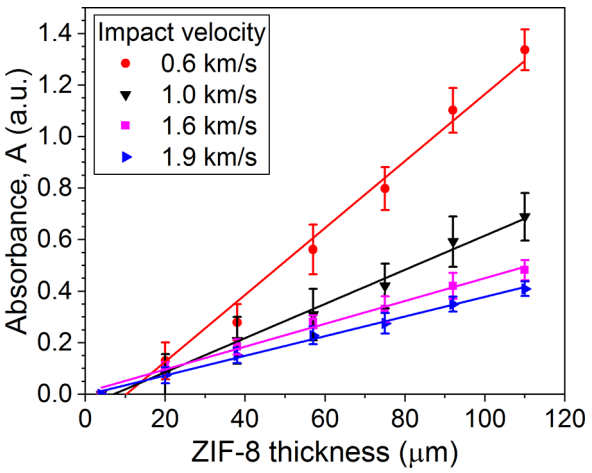

Figure 3. Shock wave energy absorbance of ZIF-8 film. The slope represents shock absorption coefficient. Error bars represent one standard deviation.

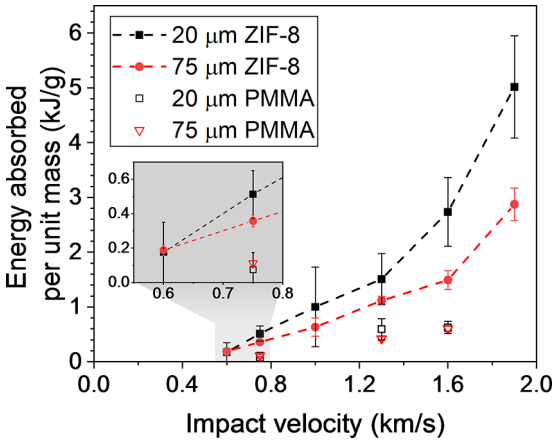

Figure 4. Shock wave energy absorbed per unit mass: a comparison between ZIF-8 and PMMA. Error bars represent one standard deviation.

shock energy absorbed per unit mass is the most useful measurement of shock wave attenuation. In Figure 4, we compare the shock energy absorbed per unit mass in ZIF-8 films with PMMA films. Refer to Supporting Information Section 12 for details. We can see that ZIF-8 films are considerably more efficient in shock energy absorption than PMMA. At 0.75 km/s, the energy absorption efficiency of 20 μm ZIF-8 is 0.51 kJ/g, about 7-fold that of the same thickness PMMA (0.074 kJ/g). At 1.6 km/s, the energy absorption efficiency of ZIF-8 at the same thickness (2.7 kJ/g) is ~4 times that of PMMA (0.63 kJ/g). In the case of 75 μm-thick materials, the ratio of energy absorption efficiency of ZIF-8 over PMMA is 3.3 at 0.75 km/s or 2.5 at 1.6 km/s. It is noteworthy that ZIF-8 displays thickness-dependent shock energy absorption efficiency, while PMMA does not. We attribute this thickness-dependency to the activation of multiple attenuation mechanisms of ZIF-8 under shock compression. ZIF-8 within the initial depth of 20 μm was always fully compacted, even at the lowest impact velocity of 0.6 km/s. Since all the three attenuation processes were activated in this case, the attenuation per unit mass was greater. As the shock wave propagated into thicker ZIF-8 layers, the shock became unable to fully compact the ZIF-8 but its energy

DOI: 10.1021/jacs.8b12905
J. Am. Chem. Soc. XXXX, XXX, XXX−XXX

could be attenuated by pore-collapse and powder-compaction, so in this case the attenuation per unit mass appeared smaller.

In summary, we have measured the dissipation of shock wave energy in polymer-bonded ZIF-8 coatings, and we studied the attenuation mechanisms by postmortem analysis of recovered shocked ZIF-8 samples. Shock waves are dissipated by the MOF film in multiple mechanisms: compaction of the MOF powder, collapse of the nanopores, and endothermic breaking of chemical bonds. Our quantitative analysis of the attenuation of the shock energy demonstrated that the shock absorbance in MOF is proportional to the ZIF-8 thickness, which allows one to determine the MOF thickness needed to attenuate an incoming shock to a desired level. We have shown that the shock energy absorbed per unit mass in ZIF-8 film is much greater than for PMMA. This research demonstrates the importance of multifunctional mechanisms to engineer improved shock wave dissipation in novel materials and composites. It is the first step in developing a predictive scientific method to understand how to produce materials that absorb shocks.

■ ASSOCIATED CONTENT

Supporting Information

The Supporting Information is available free of charge on the ACS Publications website at DOI: 10.1021/jacs.8b12905.

Experimental details, data processing details, PDV profiles, shock energy flux and fluence (PDF)

■ AUTHOR INFORMATION

Corresponding Authors

*dlott@illinois.edu

*ksuslick@illinois.edu

ORCID

Xuan Zhou: 0000-0002-4143-0248

Yu-Run Miao: 0000-0001-6429-8297

Kenneth S. Suslick: 0000-0001-5422-0701

Dana D. Dlott: 0000-0001-8719-0248

Present Addresses

†Institute for NanoBioTechnology, Johns Hopkins University, 3400 N Charles Street, Baltimore, MD 21218 (Y.-R.M.).

‡Lawrence Livermore National Laboratory, 7000 East Avenue, L-282, Livermore, CA 94551 (W.L.S.).

Notes

The authors declare no competing financial interest.

■ ACKNOWLEDGMENTS

The research described in this study was based on work supported by the Office of Naval Research under MURI grant N00014-16-1-2272. Sample preparations were carried out in part in the Frederick Seitz Materials Research Laboratory Central Facilities, University of Illinois. Sample characterizations including profilometry, SEM, and confocal Raman spectroscopy were performed in part in the Beckman Institute, University of Illinois.

■ REFERENCES

(1) Miao, Y.-R.; Su, Z.; Suslick, K. S. Energy Storage during Compression of Metal-Organic Frameworks. *J. Am. Chem. Soc.* **2017**, *139*, 4667.

(2) Ortiz, G.; Nouali, H.; Marichal, C.; Chaplais, G.; Patarin, J. Energetic Performances of the Metal-Organic Framework ZIF-8 Obtained Using High Pressure Water Intrusion-Extrusion Experiments. *Phys. Chem. Chem. Phys.* **2013**, *15*, 4888.

(3) Rodriguez, J.; Beurroies, I.; Loiseau, T.; Denoyel, R.; Llewellyn, P. L. The Direct Heat Measurement of Mechanical Energy Storage Metal-Organic Frameworks. *Angew. Chem., Int. Ed.* **2015**, *54*, 4626.

(4) Yang, K.; Zhou, G.; Xu, Q. The Elasticity of MOFs under Mechanical Pressure. *RSC Adv.* **2016**, *6*, 37506.

(5) Yot, P. G.; Vanduyfhuys, L.; Alvarez, E.; Rodriguez, J.; Itié, J.-P.; Fabry, P.; Guillou, N.; Devic, T.; Beurroies, I.; Llewellyn, P. L.; Van Speybroeck, V.; Serre, C.; Maurin, G. Mechanical Energy Storage performance of an Aluminum Fumarate Metal-Organic Framework. *Chem. Sci.* **2016**, *7*, 446.

(6) Bennett, T. D.; Tan, J.-C.; Yue, Y.; Baxter, E.; Ducati, C.; Terrill, N. J.; Yeung, H. H. M.; Zhou, Z.; Chen, W.; Henke, S.; Cheetham, A. K.; Greaves, G. N. Hybrid Glasses from Strong and Fragile Metal-Organic Framework Liquids. *Nat. Commun.* **2015**, *6*, 8079.

(7) Su, Z.; Miao, Y.-R.; Mao, S.-M.; Zhang, G.-H.; Dillon, S.; Miller, J. T.; Suslick, K. S. Compression-Induced Deformation of Individual Metal-Organic Framework Microcrystals. *J. Am. Chem. Soc.* **2015**, *137*, 1750.

(8) Kinney, G. F.; Graham, K. J. *Explosive shocks in air*, Second ed.; Springer Science + Business Media: New York, 1985.

(9) Su, Z.; Miao, Y.-R.; Zhang, G.; Miller, J. T.; Suslick, K. S. Bond Breakage under Pressure in a Metal Organic Framework. *Chem. Sci.* **2017**, *8*, 8004.

(10) Banlusan, K.; Strachan, A. Shockwave Energy Dissipation in Metal-Organic Framework MOF-5. *J. Phys. Chem. C* **2016**, *120*, 12463.

(11) Su, Z.; Shaw, W. L.; Miao, Y.-R.; You, S.; Dlott, D. D.; Suslick, K. S. Shock Wave Chemistry in a Metal-Organic Framework. *J. Am. Chem. Soc.* **2017**, *139*, 4619.

(12) Abbud, L. H.; Talib, A. R. A.; Mustapha, F.; Tawfique, H.; Najim, F. A. Behaviour of Transparant Material under High Velocity Impact. *Int. J. Mech. Mater. Eng.* **2010**, *5*, 123.

(13) Lee, J.-H.; Loya, P. E.; Lou, J.; Thomas, E. L. Dynamic Mechanical Behavior of Multilayer Graphene via Supersonic Projectile Penetration. *Science* **2014**, *346*, 1092.

(14) Kida, K.; Okita, M.; Fujita, K.; Tanaka, S.; Miyake, Y. Formation of High Crystalline ZIF-8 in an Aqueous Solution. *CrystEngComm* **2013**, *15*, 1794.

(15) Tan, J. C.; Bennett, T. D.; Cheetham, A. K. Chemical Structure, Network Topology, and Porosity Effects on the Mechanical Properties of Zeolitic Imidazolate Frameworks. *Proc. Natl. Acad. Sci. U. S. A.* **2010**, *107*, 9938.

(16) Park, K. S.; Ni, Z.; Côté, A. P.; Choi, J. Y.; Huang, R.; Uribe-Romo, F. J.; Chae, H. K.; O'Keeffe, M.; Yaghi, O. M. Exceptional Chemical and Thermal Stability of Zeolitic Imidazolate Frameworks. *Proc. Natl. Acad. Sci. U. S. A.* **2006**, *103*, 10186.

(17) Bhowmick, M.; Nissen, E. J.; Dlott, D. D. Detonation on a Tabletop: Nitromethane with High Time and Space Resolution. *J. Appl. Phys.* **2018**, *124*, No. 075901.

(18) Curtis, A. D.; Banishev, A. A.; Shaw, W. L.; Dlott, D. D. Laser-Driven Flyer Plates for Shock Compression Sciences: Launch and Target Impact Probed by Photon Doppler Velocimetry. *Rev. Sci. Instrum.* **2014**, *85*, No. 043908.

(19) Brown, K. E.; Shaw, W. L.; Zheng, X.; Dlott, D. D. Simplified Laser-Driven Flyer Plates for Shock Compression Science. *Rev. Sci. Instrum.* **2012**, *83*, 103901.

(20) Weng, J.; Wang, X.; Ma, Y.; Tan, H.; Cai, L.; Li, J.; Liu, C. A Compact All-Fiber Displacement Interferometer for Measuring the Foil Velocity Driven by Laser. *Rev. Sci. Instrum.* **2008**, *79*, 113101.

(21) Shaw, W. L.; Ren, Y.; Moore, J. S.; Dlott, D. D. Mechanochemistry for Shock Wave Energy Dissipation. *AIP Conf. Proc.* **2015**, *1793*, No. 030026.

(22) Kumari, G.; Jayaramulu, K.; Maji, T. K.; Narayana, C. Temperature Induced Structural Transformations and Gas Adsorption in the Zeolitic Imidazolate Framework ZIF-8: a Raman Study. *J. Phys. Chem. A* **2013**, *117*, 11006.

DOI: 10.1021/jacs.8b12905
J. Am. Chem. Soc. XXXX, XXX, XXX−XXX